© 2014. Published by The Company of Biologists Ltd | Journal of Cell Science (2014) 127, 1829–1839 doi:10.1242/jcs.143016

RESEARCH ARTICLE

Src kinases and ERK activate distinct responses to Stitcher receptor tyrosine kinase signaling during wound healing in *Drosophila*

Vasilios Tsarouhas*, Liqun Yao* and Christos Samakovlis‡

ABSTRACT

Metazoans have evolved efficient mechanisms for epidermal repair and survival following injury. Several cellular responses and key signaling molecules that are involved in wound healing have been identified in *Drosophila*, but the coordination of cytoskeletal rearrangements and the activation of gene expression during barrier repair are poorly understood. The Ret-like receptor tyrosine kinase (RTK) Stitcher (Stit, also known as Cad96Ca) regulates both re-epithelialization and transcriptional activation by Grainy head (Grh) to induce restoration of the extracellular barrier. Here, we describe the immediate downstream effectors of Stit signaling *in vivo*. Drk (Downstream of receptor kinase) and Src family tyrosine kinases bind to the same docking site in the Stit intracellular domain. Drk is required for the full activation of transcriptional responses but is dispensable for re-epithelialization. By contrast, Src family kinases (SFKs) control both the assembly of a contractile actin ring at the wound periphery and Grh-dependent activation of barrier-repair genes. Our analysis identifies distinct pathways mediating injury responses and reveals an RTK-dependent activation mode for Src kinases and their central functions during epidermal wound healing *in vivo*.

KEY WORDS: Drk, *Drosophila*, ERK, Src-family kinases, Stitcher, RTK signaling, Wound healing

INTRODUCTION

Epidermal injury induces a coordinated array of reactions involving epithelial, mesenchymal, endothelial and blood cells that reconstruct the damaged site. An understanding of wound responses in each cell type, and of the pathways that orchestrate the activities of different cells, is expected to advance the development of new treatments for the multiple pathologies caused by defective wound healing (Gurtner et al., 2008). *Drosophila* offers a tractable model for the molecular dissection of wound responses *in vivo* (Galko and Krasnow, 2004; Razzell et al., 2011). Epidermal cells in wounded embryos rapidly migrate and assemble an actin-rich ring around the wound that constricts and closes the gap. Wounding also initiates inflammation and activates ERK to induce the expression of barrier-repair genes in epithelial cells at the wound site (Mace et al., 2005; Pearson et al., 2009; Wood et al., 2006). The evolutionarily conserved transcription factor Grainy head (Grh) is phosphorylated by ERK and lies at the heart of wound healing (Kim and McGinnis, 2011). It activates the barrier-repair genes *Dopa decarboxylase* (*Ddc*) and *pale* (*ple*, encoding tyrosine hydroxylase) in *Drosophila* and transglutaminase-1 in mice (Ting et al., 2005; Wang and Samakovlis, 2012). *Stitcher* (*stit*, also known as *Cad96Ca*) encodes a Ret-family receptor tyrosine kinase (RTK), which is also activated by Grh following wounding. Live-imaging analysis of wounded *stit* embryos reveals that Stit promotes actin-cable assembly during re-epithelialization after wounding. Stit also triggers ERK activation at the injury site, leading to a Grh-dependent upregulation of wound-repair genes and of its own transcription. Thus, Stit activation is crucial for the activation of epidermal wound responses in embryos (Wang et al., 2009). Additionally, embryos with mutations in the genes encoding either the *Drosophila* epidermal growth factor receptor ($EGFR^{t1}$) or the ERK homolog $rolled^{10a}$ show defective wound closure (Geiger et al., 2011). In *Drosophila* larvae, the Platelet-derived growth factor and vascular endothelial growth factor (PDGF and VEFG) receptor (Pvr) is required for wound closure. This RTK becomes activated by its ligand Pvf1 upon epithelial disruption and induces actin polymerization and wound closure. Thus, genetic analysis in flies has identified three different RTKs that are required for epithelial-wound closure at different developmental stages. Numerous signal transducers including Ca^{2+} (Razzell et al., 2013), the Rho family of GTPases (Wood et al., 2002), ERK (Geiger et al., 2011; Mace et al., 2005) and JNK (Galko and Krasnow, 2004; Rämet et al., 2002) orchestrate the activation of transcriptional and cytoskeletal wound responses. Recent genetic screens for mutants with defective wound closure have rapidly expanded the catalog of new signaling molecules and effectors of wound healing in flies (Campos et al., 2010; Juarez et al., 2011; Lesch et al., 2010). However, a mechanistic view of the links and regulatory relationships between the different components of wound-healing responses is still missing.

RTK signaling plays prominent roles during wound re-epithelialization in vertebrates as well as in *Drosophila*. Several RTKs become activated after injury to control epithelial migration and wound closure (Müller et al., 2012). Conditional inactivation of hepatocyte growth factor (HGF, also known as scatter factor) receptor (c-Met) in keratinocytes abolishes the migratory capacity of these cells during wound re-epithelialization. This is accompanied by a decrease in the phosphorylation of ERK and other kinases, and a failure in cytoskeletal rearrangement in response to HGF (Chmielowiec et al., 2007). Simultaneous inactivation of two other RTKs, the fibroblast growth factor

Department of Molecular Biosciences, The Wenner-Gren Institute, Stockholm University, S-10691 Stockholm, Sweden.
*These authors contributed equally to this work

‡Author for correspondence (christos.samakovlis@su.se)

Received 19 September 2013; Accepted 6 January 2014

Journal of Cell Science

Journal of Cell Science (2014) 127, 1829–1839 doi:10.1242/jcs.143016

receptors FGFR1 (isoform IIIb) and FGFR2 (isoform IIIb) also delays wound healing and keratinocyte migration. In this case, cell adhesion and the expression of focal adhesion kinase and paxillin were reduced in the mutants (Meyer et al., 2012). Recent studies in zebrafish revealed a direct role for Fynb [an intracellular transducer of the Src family kinases (SFKs)] and Ca^{2+} signaling in the early events of regeneration of amputated fins. In this system, ERK activation is required in parallel with Fynb for regeneration, and the two signal transducers might share downstream effectors (Yoo et al., 2012). Collectively, research in several model organisms has identified several RTKs and signal transducers that control epithelial wound responses. To understand the mechanisms of RTK functions in epidermal wound healing, we dissected Stit signaling and its signal transducers after wounding in *Drosophila* embryos.

RESULTS

Mapping of phosphorylated tyrosine residues on the intracellular domain of Stit

RTKs become auto-phosphorylated upon ligand-induced dimerization, and these phosphorylation events are necessary for the activation of downstream effectors (Lemmon and Schlessinger, 2010). We searched for putative tyrosine (Y) phosphorylation sites in the intracellular domain of Stitcher (http://www.cbs.dtu.dk/services/NetPhos/). Four of the six predicted phospho-tyrosine (pY) residues resided in the kinase domain and two were in the C-terminal tail domain (Fig. 1A). Sequence alignments of Stit-like proteins from multiple species revealed the conservation of five of these six residues across a range of insect species (supplementary material Fig. S1A). To investigate whether these residues become auto-phosphorylated upon Stit overexpression, we generated V5-tagged Stit constructs by either replacing each single tyrosine residue with a non-phosphorylatable phenylalanine (F), by altering the four residues in the kinase domain ($Stit^{Kinase\ Quad}$) or by replacing all six tyrosine residues ($Stit^{Hex}$) (Fig. 1B). We overexpressed these constructs along with a wild-type and a kinase-dead form of Stit [$Stit^{KD}$, in which lysine 504 is replaced with alanine (K504A)] (Wang et al., 2009) in S2 cells. Following immunoprecipitation of the Stit proteins with anti-V5 antibodies, we probed western blots with an anti-pY antibody to assess the phosphorylation levels of each protein construct. As expected, wild-type Stit became heavily phosphorylated when it was overexpressed, and the pY signal was abolished in the $Stit^{KD}$ mutant form, indicating that Stit kinase activity is essential for auto-phosphorylation of the tyrosine residues of the intracellular domain. Whereas single tyrosine substitutions did not affect pY signal intensity (data not shown), we detected a severe reduction in the signal in $Stit^{Kinase\ Quad}$. This suggested that tyrosine residues in both the kinase domain and in the cytoplasmic tail are phosphorylated. The phosphorylation level of $Stit^{Hex}$ was much reduced compared with the $Stit^{Kinase\ Quad}$ control, and it was comparable to the kinase-dead control (Fig. 1C). This indicates that the Y751 and Y762 residues in the tail domain are phosphorylated upon Stit activation by overexpression. In summary, this analysis of the constructs indicates that the six predicted pYs account for most, if not all, Stit phosphorylation sites.

Identification of Stit-binding partners

To identify Stit signal transducers, we performed a yeast two-hybrid screen using the intracellular domain of Stit as bait. By screening a prey library of 72 million clones, we identified 185 interacting clones. We focused on four unique binding partners; Drk (Downstream of receptor kinase), Src42A, Src64B and Btk29A. Each of these possessed a Src homology 2 (SH2) domain that specifically recognizes pY (Sadowski et al., 1986), and each was represented by multiple interacting clones (supplementary material Fig. S1B). Drk, a homolog of mammalian GRB2, contains an SH2 and two SH3 domains that couple activated RTKs to the Ras guanidine exchange factor Sos (Olivier et al., 1993), which further activates the Ras1–MAPK pathway in flies. Src42A and Src64B are the closest *Drosophila* relatives of the Src oncogene product, the defining member of the SH2 and SH3 family of proteins (Takahashi et al., 1996). The gene *btk29A* (also known as *tec29*) also encodes non-receptor tyrosine kinases (Lu et al., 2004) (supplementary material Fig. S1B). Members of the Src family and Btk29A often act together to regulate epithelial proliferation and morphogenesis (Shindo et al., 2008; Tateno et al., 2000; Vidal et al., 2007; Wouda et al., 2008).

In another assay to investigate whether the putative Stit effectors bind to phospho-Stit, we produced GST-tagged versions of the SH2 domains of Drk, Src42A and Src64B in bacteria, and tested their binding to V5-tagged Stit versions produced in S2 cells. All three GST–SH2 fusions bound to wild-type Stit but only showed very weak association with the inactive $Stit^{KD}$ form (Fig. 2A–C). This indicates that the three effectors selectively bind to phosphorylated Stit.

Y762 is an essential docking site for Stit signal transduction

We further tested which tyrosine residue mediates Stit binding to the SH2 domains of the three binding partners. We produced six V5-tagged Stit versions, each replacing one of the six predicted pYs, and one construct substituting phenylalanine residues for the two C-terminal tail pYs. All Stit versions apart from the ones lacking kinase activity ($Stit^{KD}$) or replacing Y^{762} ($Stit^{Y762F}$ and $Stit^{Y751F,\ Y762F}$) showed strong binding to the SH2-domains of Drk, Src42A and Src64B (Fig. 2A–C). This indicates that Y^{762} is crucial for Stit binding to Drk and to SFKs. We next tested the significance of Y^{762} for Stit function *in vivo*. Mutants that are null for *stit* die at late pupal stages. This phenotype can be partially rescued by transgenic expression of wild-type Stit, but not by $Stit^{KD}$, in ectodermal tissues of *stit* mutants (Wang et al., 2009). We generated *stit* mutants expressing similar levels of either wild-type Stit, or $Stit^{KD}$ or $Stit^{Y762F}$ transgenes (Fig. 2E), and scored adult survival. Whereas the wild-type Stit enabled survival in 39% of *stit* mutants, the $Stit^{Y762F}$ version only rescued lethality in 6% of the mutants (Fig. 2D). Thus, Y^{762} provides the major binding site for Stit effectors and has a crucial function in Stit signaling *in vivo*.

stit mutants show reduced diphosphorylated (dp)ERK accumulation at the wound site, and Stit overexpression induces ectopic ERK activation (Wang et al., 2009). To test the requirement for Y^{762} in ERK activation, we compared the abilities of Stit and $Stit^{Y762F}$ to induce dpERK accumulation. Upon overexpression in epidermal stripes, $Stit^{Y762F}$ only induced a weak accumulation of dpERK in the expressing cells compared with the robust increase in the dpERK signal induced by Stit (Fig. 3A–B″). This indicates that Y762 is crucial for ERK activation. ERK phosphorylation following wounding leads to transcriptional activation of wound reporter genes. To investigate the impact of Y762 on the activation of the 1.4-kb *Ddc1.4*-GFP transcriptional reporter (Mace et al., 2005), we expressed $Stit^{Y762F}$ and a $Stit^{Y751F}$ version, which retains the ability to bind to Drk and Src. Consistent with its failure to activate ERK, overexpression of

Journal of Cell Science (2014) 127, 1829–1839 doi:10.1242/jcs.143016

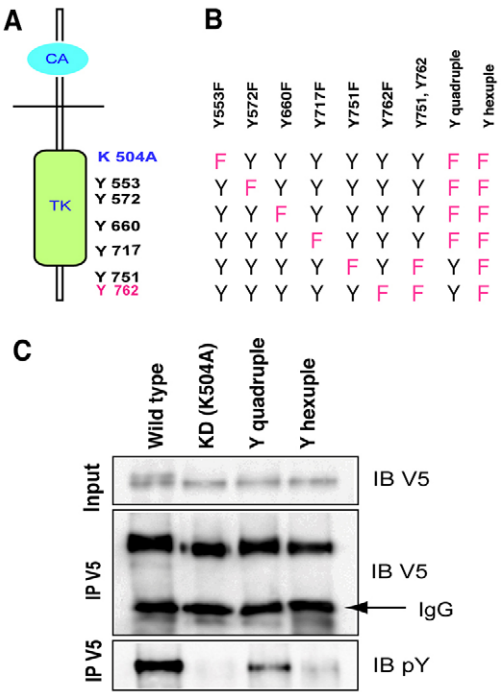

Fig. 1. Tyrosine phosphorylation sites on Stit. (A) Schematic of the Stit domains including predicted phosphorylation sites. Four of the six putative tyrosine phosphorylation sites fall in the kinase domain, whereas two are present in the tail domain. K504, identified previously as the lysine required for kinase activity, is indicated in blue, and the physiologically relevant residue Y762 is indicated in magenta. CA, cadherin domain; TK, tyrosine kinase domain. (B) Table showing a summary of the tyrosine to phenylalanine mutations used in this study (magenta). (C) Western blot showing immunoprecipitated (IP) V5-tagged, wild-type and mutant versions of Stit expressed in S2 cells. Upper panel, the quantification of input protein levels probed with an anti-V5 antibody. Middle panel, protein levels in the immunoprecipitates probed with an anti-V5 antibody. Lower panel, the immunoprecipitates probed with an anti-pY antibody to reveal the phosphorylation levels of the constructs. The arrow indicates the irrelevant IgG band recognized by the secondary antibody. KD, kinase dead.

Stit^{Y762F} did not activate *Ddc1.4*-GFP, whereas overexpression of Stit^{Y751F} readily induced it (Fig. 3C,C′). Thus, Y^{762} has a key role in ERK phosphorylation and the activation of the reporter.

Drk is required downstream of Stit for activation of wound-response genes

The Drk adaptor binds to phosphorylated RTKs and activates the Ras–Raf–Mek pathway, which culminates in the dual phosphorylation of ERK (Gabay et al., 1997). We hypothesized that Drk binding to Y^{762} on Stit leads to ERK phosphorylation and the transcriptional induction of injury repair genes. We first tested whether *drk*^{eOA} mutants (Simon et al., 1991) could activate *Ddc1.4*-GFP following wounding. This reporter faithfully reflects the rapid accumulation of *Ddc* transcripts at the wound sites of wild-type embryos (Mace et al., 2005). However, both *Ddc* mRNA and the *Ddc1.4*-GFP reporter were also expressed in the epidermis of unwounded stage 17 embryos, reflecting the developmental maturation of the epidermal barrier (supplementary material Fig. S2A–C; Movie 1). To elucidate the wound-response-specific roles of Drk and the other Stit effectors, we performed our injury assays during a defined interval prior to the developmental activation of *Ddc1.4*-GFP (supplementary material Fig. S2C,D; Movie 2). Following injury, 82% of the control embryos showed a broad strong *Ddc1.4*-GFP induction around the wound site. Only 17% of *drk*^{eOA} mutants showed comparable wound-induced *Ddc1.4*-GFP activation. Moreover, 39% of *drk*^{eOA} mutants showed a very weak induction of the reporter as opposed to 3% of control embryos (Fig. 4A–C). This weak activation of *Ddc1.4*-GFP after injury in *drk*^{eOA} mutants resembles the *stit* mutant phenotypes (Wang et al., 2009), and suggests that Drk is required downstream of Stit for the full activation of gene expression upon epidermal wounding. We further investigated the potential requirement of Drk in the transcriptional activation of *Ddc* by Stit signaling. We overexpressed *Stit* by using the *en*Gal4 driver, and detected *Ddc* transcripts by *in situ* hybridization. *Stit* overexpression induced ectopic *Ddc* mRNA accumulation in epidermal stripes and in regions of the hindgut compared with wild-type embryos at stage 16. This ectopic *Ddc* expression was not detected in *drk*^{eOA} mutants overexpressing *stit* by the same driver (Fig. 4D), indicating that Drk is required downstream of Stit for the activation of wound-response genes.

To investigate whether Drk is also required for Stit signaling leading to re-epithelialization, we recorded wound closure in wild-type and *drk*^{eOA} mutant embryos expressing the *spaghetti-squash*-Moesin–GFP (sGMCA) reporter (Kiehart et al., 2000). We inflicted laser wounds to stage-15 control and *drk*^{eOA} embryos and monitored their closure. The epidermal cells in both the control and *drk*^{eOA} mutant embryos readily extended over the gap and closed it. Wound closure was completed in average within 161.5 min in wild-type embryos ($n=18$) and within 176 min in *drk*^{eOA} mutants ($n=13$) (supplementary material Fig. S3A). This minor delay in re-epithelialization contrasts with the notable reduction of *Ddc1.4*-GFP activation in *drk*^{eOA} mutants and suggests that Drk binding to activated Stit predominantly induces transcriptional activation of wound-response genes without influencing the cytoskeleton.

Src-family kinases and Btk control the assembly of a continuous actin ring during wound closure

To elucidate how Stit signaling controls multiple responses in epidermal cells following wounding, we investigated the function of its remaining binding partners. We visualized wound closure in laser-wounded wild-type and *src42A*^{E1} mutant embryos (Laberge et al., 2005), by using the sGMCA reporter at stage 15. Whereas all control embryos closed their wounds within ~141 min, 19% of *src42A*^{E1} mutants failed to heal within the 8-h period of imaging and the remaining *src42A*^{E1} mutants showed delayed re-epithelialization, with a mean wound-closure time of 202 min (Fig. 5A). This suggests that Src42A is required for efficient wound re-epithelialization. By contrast, wounded *btk29A*^{206} and *src64B* single mutants expressing the sGMCA reporter repaired their epidermal wounds as efficiently as control embryos treated in parallel (supplementary material Fig. S3B,C). To assess whether the loss of Btk29A or Src64B could exacerbate the wound-closure defects of *src42A*^{E1} mutants, we generated *src42A*^{E1} *btk29A*^{206} and *src42A*^{E1} *src64B* double mutants expressing the sGMCA marker. To avoid indirect effects caused by the developmental role of Src-like kinases in dorsal closure, we inflicted wounds in the ventral epidermis, the integrity of which is not affected in the double mutants (Tateno et al., 2000). Whereas 93% of wild-type embryos completely closed their wound within 166 min, only 40% of *src42A*^{E1} *btk29A*^{206} double mutants managed to do so (Fig. 5A′). The average closure time

Journal of Cell Science (2014) 127, 1829–1839 doi:10.1242/jcs.143016

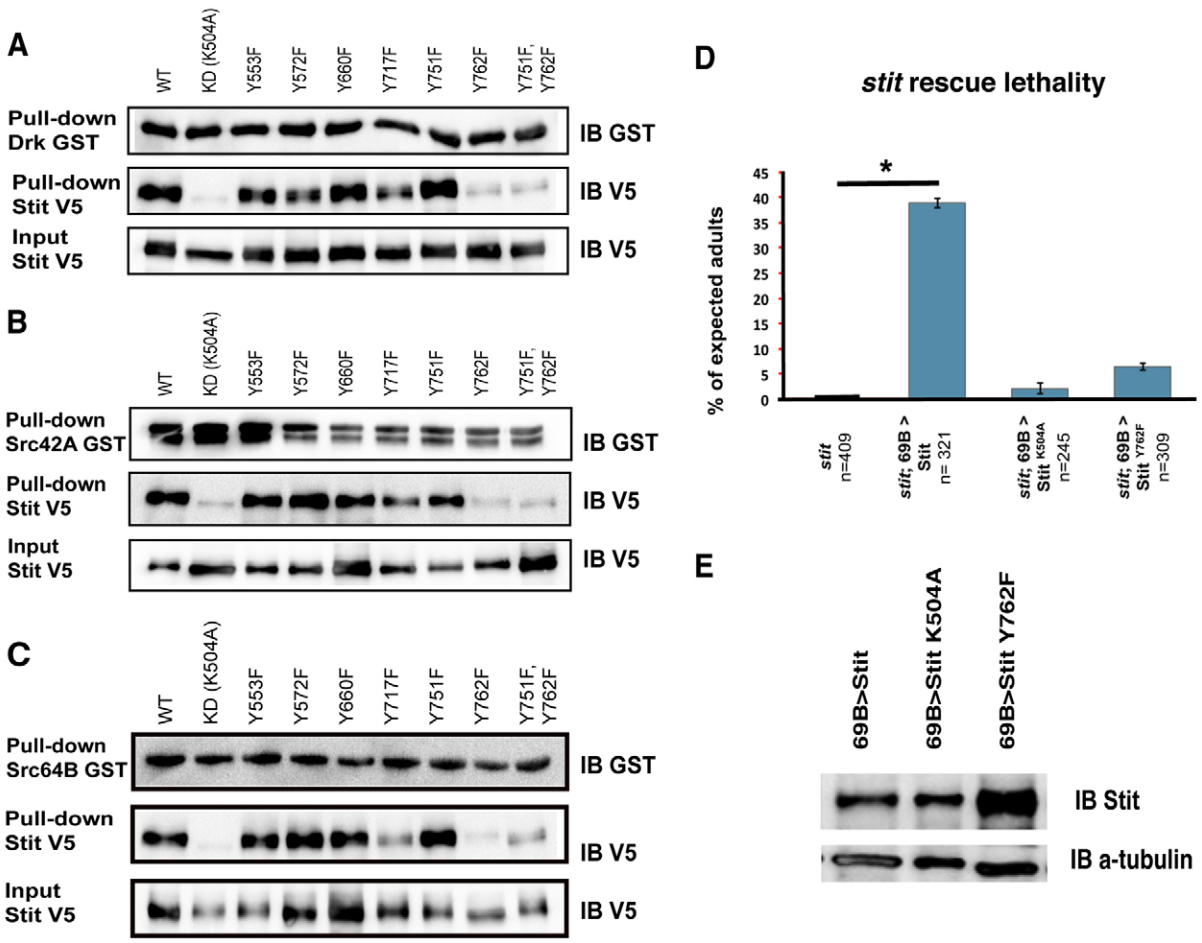

Fig. 2. Stit kinase activity and tyrosine Y762 are required for Stit binding to the SH2 domains of its partners, and for Stit function *in vivo*. (A) Stit and Drk interact *in vitro* through Y762. GST pull-downs showing binding of bacterial SH2-Drk–GST to wild-type and mutated forms of Stit–V5 from S2 cell lysates. Upper panel, the levels of the pulled-down fractions of SH2-Drk–GST. Middle panel, the levels of Stit variants bound to SH2-Drk–GST. SH2-Drk binding is dependent on the residue responsible for Stit kinase activity, K504, and on Y762. Lower panel, the relative amounts of Stit–V5 used for immunoprecipitation. (B) Stit and Src42 interact *in vitro* through Y762. GST pull-downs showing binding of bacterial SH2-Src42–GST to wild-type and mutated forms of Stit–V5 from S2 cell lysates. Upper panel, the levels of the pulled-down fractions of SH2-Src42–GST. Middle panel, the levels of Stit variants bound to SH2-Src42–GST. Binding to SH2-Src42 is dependent on the Stit residues K504 and Y762. Lower panel, the amounts of Stit–V5 loaded on the resin. (C) Stit and Scr64B interact *in vitro*, and this interaction occurs predominantly through Y762. GST pull-downs of bacterial SH2-Src64B–GST, incubated with the different versions of Stit–V5 that were expressed in S2 cells. Upper panel, the levels of pull-down of SH2-Src42–GST. Middle panel, the levels of Stit variants bound to SH2-Src64–GST. SH2-Src64 binding is also dependent on the Stit residues K504 and on Y762. Lower panel, the relative amounts of Stit–V5 used for immunoprecipitation. (D) Phenotypic analysis of the relative rescue activity of Stit constructs. $Stit^{WT}$, $Stit^{K504A}$ and $Stit^{Y762F}$ were expressed using *69B*-Gal4 in *stit* mutant flies and enclosed adults of *stit* mutants were counted. The graph shows the percentage of the expected adults if the rescue activity of each construct was 100%. *n*, number of adults enclosed. Results show means±s.e.m. (three independent experiments). **P*<0.0005, two-tailed Student's *t*-test. (E) Western blot showing the relative Stit protein levels (upper panel) in transgenic lines $Stit^{WT}$, $Stit^{K504A}$ and $Stit^{Y762F}$ using the *69B*-Gal4. Extracts were prepared from embryos at 14–15 h after egg laying. α-Tubulin (lower panel) was used as a loading control.

for the remaining $src42A^{E1}$ $btk29A^{206}$ mutants was 395 min, twice as long as control embryos. Similarly, in $src42A^{E1}$ *src64B* double mutants expressing the sGMCA marker, 50% of the embryos failed to close their wounds and the remaining mutant embryos showed a significant delay in wound closure compared with the control (supplementary material Fig. S3D). This suggested that Src42A, Src64B and Btk29A collectively mediate epidermal wound closure. To investigate which aspect of re-epithelialization requires the function of non-receptor tyrosine kinases, we imaged wound closure in control, $src42A^{E1}$, $src42A^{E1}$ *src64B* and $src42A^{E1}$ $btk29A^{206}$ embryos by confocal microscopy. We did not detect gross differences in the cellular protrusions of the leading cells at the wound edges between the mutant and control embryos. However, the actin ring surrounding and closing the wound in wild-type embryos was discontinuous in $src42A^{E1}$ mutants and failed to form in the $src42A^{E1}$ $btk29A^{206}$ and $src42A^{E1}$ *src64B* double mutants (Fig. 5B–D; supplementary material Fig. S3E,E′; Movies 3,4). We compared the relative fluorescence intensity (RFI) of sGMCA at the wound perimeter at different timepoints during wound healing in control, $src42A^{E1}$, $src42A^{E1}$ $btk29A^{206}$ and $src42A^{E1}$ *src64B* mutants. The relative signal intensity of the actin-filament marker around the wound perimeter rose sharply during the entire process, both in controls and $src42A^{E1}$, but failed to reach its peak in $src42A^{E1}$ mutants. By contrast, the actin-cable RFI in double mutants remained flat during the entire wound-healing process (Fig. 5E). This suggested that Src42A, Src64B and Btk29A act collectively to establish and maintain the actin ring at the wound perimeter. We

Journal of Cell Science (2014) 127, 1829–1839 doi:10.1242/jcs.143016

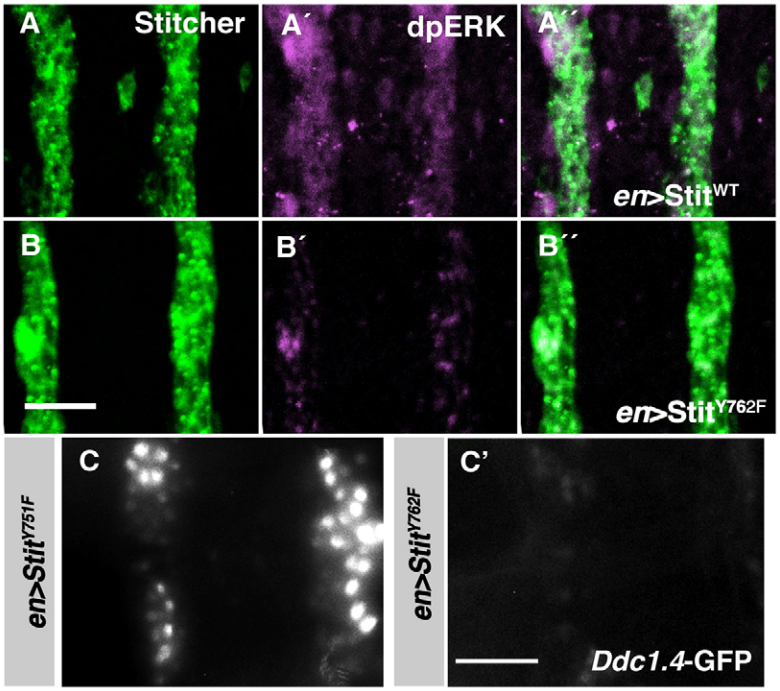

Fig. 3. Tyrosine Y762 of Stit is essential for dpERK and *Ddc1.4*-GFP induction. (A–B″) Confocal projections of wild-type embryos expressing *en*>Stit^{WT} (A–A″) and *en*>Stit^{Y762F} (B–B″). Embryos were stained with anti-dpERK (magenta) and anti-Stit (green). Ectopic dpERK activation by *en*>Stit^{Y762F} embryos (B–B″) was drastically reduced compared with *en*>Stit^{WT}. The two Stit constructs were expressed at similar levels (green). (C,C′) *Ddc1.4*-GFP is ectopically activated in stripes by *en*>Stit^{Y751F} (C) but not by *en*>Stit^{Y762F} (C′). Scale bars: 20 µm.

conclude that the SFKs bind to phosphorylated Stit and are required, like Stit (Wang et al., 2009), for intercellular actin-ring formation and re-epithelialization following wounding.

Src activates wound-response genes upon Stit signaling

We further tested whether Src kinases are also required downstream of Stit for transcriptional activation of wound-response genes. We compared the induction of the *Ddc1.4*-GFP and *ple*-DsRed transcriptional wound reporters in wild-type and *src42A*^{E1} mutant embryos at 3 h post-injury. Wounding induced a broad strong *Ddc1.4*-GFP response in 75% of wild-type embryos. The remainder of these embryos showed a moderate increase in GFP in the cells surrounding the injury site (Fig. 6A,C). However, *src42A*^{E1} mutants showed a reduced GFP induction (Fig. 6A′). Only 23% of the mutants showed strong and broad GFP accumulation at the wound site, whereas 37% showed a moderate induction and 40% displayed a weak and limited GFP accumulation at the wound (Fig. 6C). In contrast to *src42A* mutant embryos, *src64B* mutants did not show any significant reduction in the activation of the *Ddc1.4*-GFP reporter after wounding compared with control embryos (supplementary material Fig. S3F). This suggested that Src64B is dispensable for the activation of *Ddc* upon wounding. *src42A*^{E1}

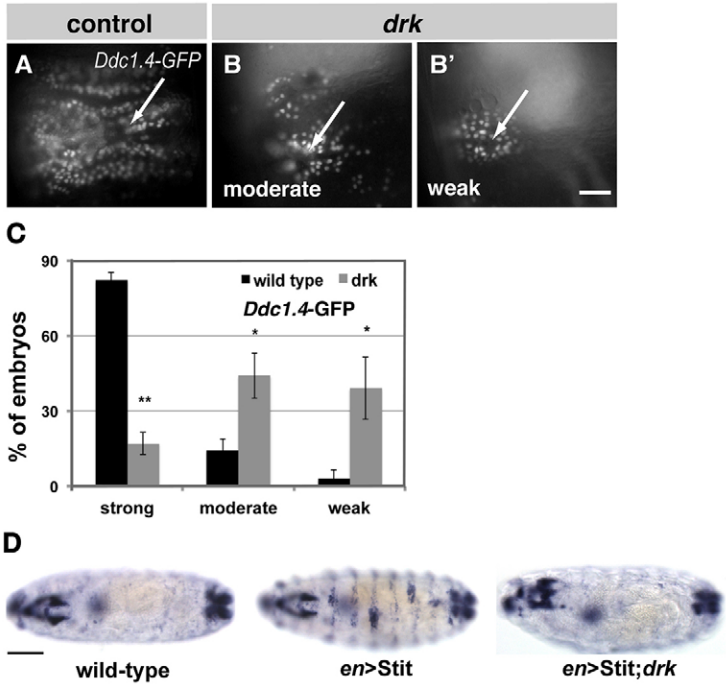

Fig. 4. Drk is required for wound-reporter activation following injury and Stit overexpression. (A–B′) *Ddc1.4*-GFP reporter induction is reduced in wounded *drk* mutants (B,B′) compared with control embryos (A). *drk* mutants displayed predominantly moderate (B) or weak (B′) wound-reporter induction. Induction was recorded 3 h post-wounding. Arrows mark the wound site. Scale bar: 30 µm. (C) Quantification of *Ddc1.4*-GFP reporter induction in wounded control (wild type, $n=131$) and *drk* mutant ($n=132$) embryos. *Ddc1.4*-GFP induction was classified as strong, moderate or weak based on the extent of GFP at the wound site. Results show means±s.e.m. (three independent experiments). *$P<0.05$, **$P<0.005$. (D) *Ddc* induction in wild-type, *en*>Stit and *en*>Stit;*drk* embryos detected by mRNA *in situ* hybridization. Upregulation of *Ddc* is detected in epidermal stripes and in the hindgut upon Stit^{wt} overexpression (middle panel), but is lost in *drk* mutants expressing Stit^{wt} with the same driver strain (right panel). Scale bars: 100 µm.

Journal of Cell Science (2014) 127, 1829–1839 doi:10.1242/jcs.143016

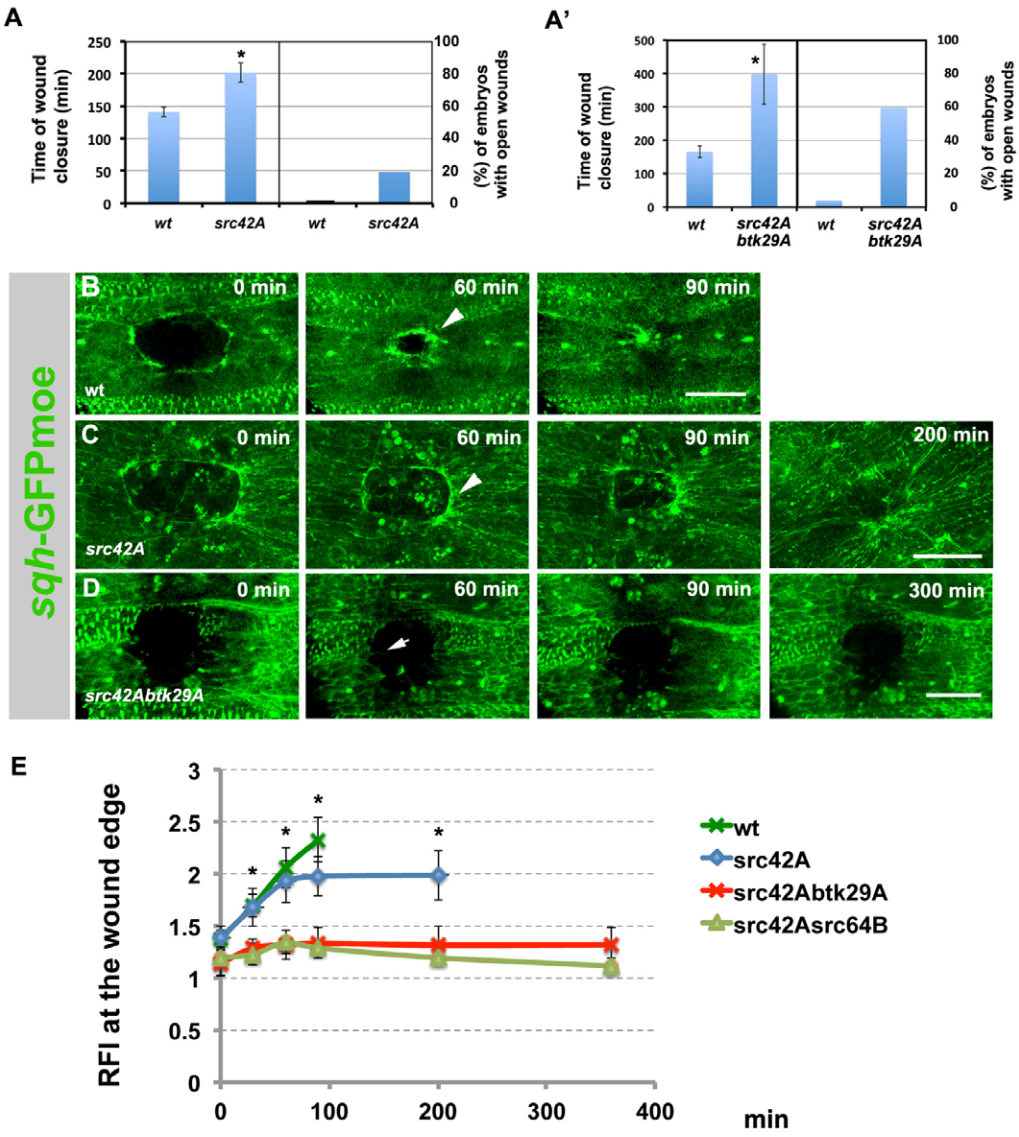

Fig. 5. Src kinases are required for actin-cable assembly around the wound edge and re-epithelialization after wounding. (A,A′) Quantification of the time taken for wound closure (min) and the percentage of embryos with open wounds in wild-type, *src42A* mutant and *src42A btk29A* mutant embryos. (A) *src42A* mutant embryos (n=21) closed their wounds with 1 h delay (on average) compared with wild type (n=24), whereas 19% of the wounded *src42A* embryos failed to close wounds. (A′) *src42A btk29A* mutant embryos (n=22) sealed their wounds ~4 h later (on average) compared with wild-type (n=21). 59% of the wounded *src42A btk29A* embryos had open wounds for at least 8 h. Results show means±s.e.m. *P<0.005 (six independent experiments). (B–D) Confocal time-lapse images of epidermal wounds in wild-type (B), *src42A* (C) and *src42A btk29A* (D) embryos expressing *sqh*-GFP–moe. Wild-type and *src42A* embryos form a strong actin cable (arrowheads) around the wound edge (B,C). In *src42A btk29A* mutants, *sqh*-GFP–moe is drastically reduced at the wound edges. (D) Actin-rich protrusions (arrow) towards the wound center are present in double mutants. Scale bars: 20 µm. (E) Plot of changes in relative fluorescence intensity (RFI) of GFP–moe at wound edges in wild-type (n=12, dark green), *src42A* (n=8, blue), *src42A btk29A* (n=10, red) and *src42A src64B* (n=4, light green) embryos. RFIs were calculated at defined points during the average wound-closure time. RFI is significantly lower in double mutants compared with wild type and the *src42A* mutant. Results show means±s.e.m. *P<0.001 compared with the initial time-point (paired two-tailed Student's t-test).

mutants also showed a defect in the activation of *ple*-DsRed following injury (Fig. 6B,B′,D), suggesting that Src42A is required for the transcriptional induction of several barrier-repair genes after injury. To extend the analysis of the role of Src42A in gene activation downstream of Stit, beyond the level of wound reporters, we overexpressed *stit* in epidermal stripes in *src42A* mutants and wild-type control embryos, and analyzed the expression of *Ddc* mRNA. Control embryos expressing Stit under the control of *en*GAL4 showed the anticipated ectopic accumulation of *Ddc* mRNA in epidermal stripes at late stage 16. However, $src42A^{E1}$ mutants expressing *stit* under the control of the same driver did not show any ectopic *Ddc* expression (Fig. 6E–E″). This indicates that Src42A is required downstream of Stit for *Ddc* activation. Interestingly, we observed that $src42A^{E1}$ embryos at late stage 16 showed conspicuous patches of *Ddc*-expressing cells in the dorsal epidermis (Fig. 6E′″). This ectopic activation of *Ddc* in $src42A^{E1}$ mutants is Stit-independent, because it was also detected in $src42A^{E1}$ mutant embryos lacking the *UAS-stit* transgene. In 80% of unwounded $src42A^{E1}$ mutants (n=34), there was widespread *Ddc* mRNA signal in the dorsal epidermis around the site of the failed dorsal closure at late stage 16 (supplementary material Fig. S4A,B). Consistently, the *Ddc1.4*-GFP marker became upregulated in the

Journal of Cell Science (2014) 127, 1829–1839 doi:10.1242/jcs.143016

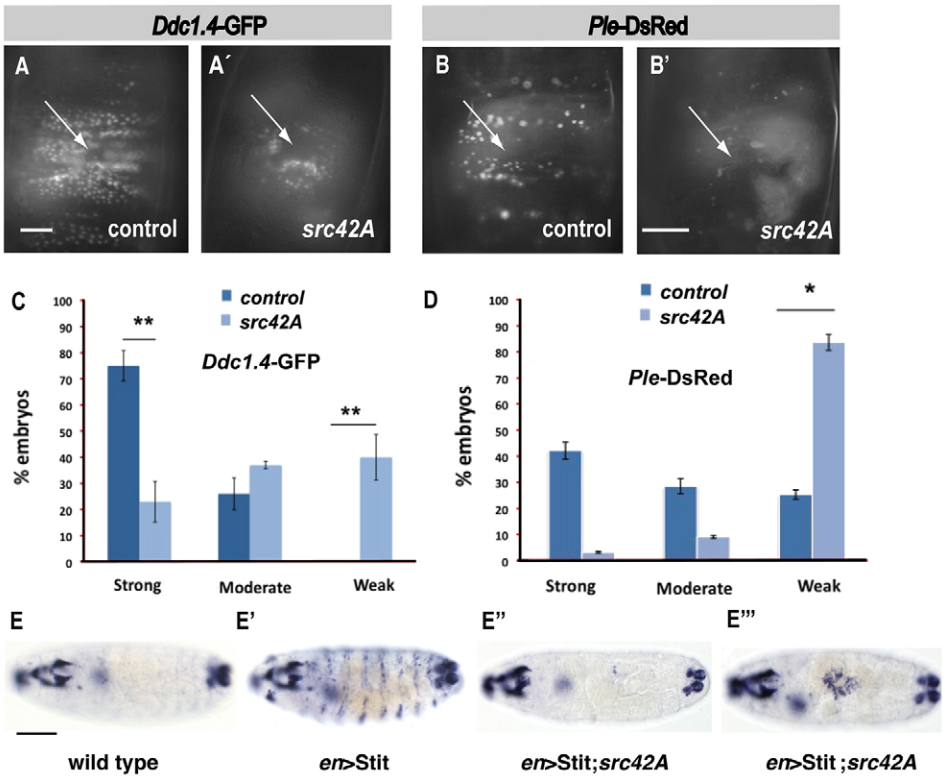

Fig. 6. Src42A is required for the induction of wound reporters and for *Ddc* activation downstream of Stit. (A,A′) Wound induction of *Ddc1.4*-GFP in control (A) and *src42A* mutant embryos (A′). *Ddc1.4*-GFP induction is reduced in *src42A* mutant embryos (A′) compared with control wounded embryos (*Ddc1.4*-GFP) (A). Induction was imaged 3 h post-wounding. Arrows mark the wound site. Scale bar: 30 µm. (B,B′) *Ple*-DsRed reporter induction in wounded control (*Ple*-DsRed) (B) and *src42A* mutant embryos (B′). *Ple*-DsRed induction in *src42A* mutant wounded embryos is reduced compared with control (*Ple*-DsRed). Induction was recorded at 3 h post-wounding. Arrows mark the wound site. Scale bar: 30 µm. (C) Quantification of the induction of the *Ddc1.4*-GFP reporter in wounded control (n=82) and *src42A* mutant (n=83) embryos. *Ddc1.4*-GFP induction is classified as strong, moderate or weak based on the extent of GFP at the wound site. The *y*-axis shows the percentage of embryos in each phenotypic category. Data show the mean±s.e.m. (three independent experiments). **P<0.005. (D) Quantification of the induction of the *Ple*-DsRed reporter in wounded control (n=64) and *src42A* mutant (n=64) embryos. *Ple*-DsRed expression is classified as strong, moderate or weak based on the extent of DsRed signals at the wound site. The *y*-axis shows the percentage of embryos displaying each phenotype. Data show the mean±s.e.m. (three independent experiments). *P<0.05. (E–E‴). *In situ* hybridization of wild-type (E), *en*>Stit (E′) and *en*>Stit; *src42A* (E″,E‴) embryos. The induced *Ddc* expression that is detected following Stit^{wt} overexpression is drastically reduced in the *src42A* mutant. Occasionally, *en*>Stit; *src42A* mutant embryos show dorsal-closure defects accompanied by *Ddc* mRNA accumulation at the edges of the apposing epidermal sheets (E‴). Scale bar: 100 µm.

dorsal epidermis of *src42A*^{E1} embryos at late stage 16 (supplementary material Fig. S4C,D). This suggests an additional developmental role of Src42A in restricting the epidermal expression of *Ddc*.

We further analyzed the activation of *Ddc1.4*-GFP in *src42A*^{E1} *btk29A*^{206} double mutants to investigate whether Btk29A also contributes to the activation of wound-response genes following injury. Consistent with the developmental roles of Src42A and Btk29A in the embryonic epidermis (Tateno et al., 2000), the expression of the *Ddc1.4*-GFP marker was increased in the dorsal epidermis of unwounded *src42A*^{E1} *btk29A*^{206} double mutants (supplementary material Fig. S4E). However, we did not detect any further reduction in GFP activation following wounding in the ventral epidermis of the double *src42A*^{E1} *btk29A*^{206} mutants compared with the decrease observed in *src42A*^{E1} embryos (supplementary material Fig. S4F–G). This suggests that among the non-receptor tyrosine kinases, Src42A is the prominent activator of *Ddc* expression after wounding. Collectively, our analysis suggests that Src42A and Btk29A have distinct effects on *Ddc* expression during epidermal morphogenesis and wound healing. During late embryogenesis, they are both required to restrict the developmental expression of *Ddc* independently of Stit signaling and injury. Following injury or Stit activation, Src42A is required to activate wound-response genes at the wound site.

Src42A activation of gene expression requires Grh

The function of Src42A in the initiation of gene expression after wounding prompted us to investigate the transcription factors downstream of Src. The activity of Src kinases is controlled by phosphorylation. Csk phosphorylates Src on Y^{527}, leading to an intermolecular interaction that keeps Src in an auto-inhibitory conformation. The substitution of a phenylalanine residue for Y^{527} in Src42A generates a constitutively active form (Src42A^{CA}), because it relieves this negative regulation (Nada et al., 1991). We expressed Src42A^{CA} either in lateral epidermal stripes using *en*-GAL4, or in the dorsal epidermis using *pnr*-GAL4, and asked whether Src42A^{CA} is sufficient to induce the transcriptional activation of wound reporters. Both the barrier-repair marker *Ddc1.4*-GFP and the *stitγ* wound reporter (Wang et al., 2009) were readily activated in Src42A^{CA}-expressing cells in the epidermis of unwounded embryos (Fig. 7A,B–C). This indicates that Src42A activation is sufficient to induce wound-response genes. We then asked whether Grh mediates the transcriptional activation of wound reporters by Src42A^{CA}. In

Journal of Cell Science (2014) 127, 1829–1839 doi:10.1242/jcs.143016

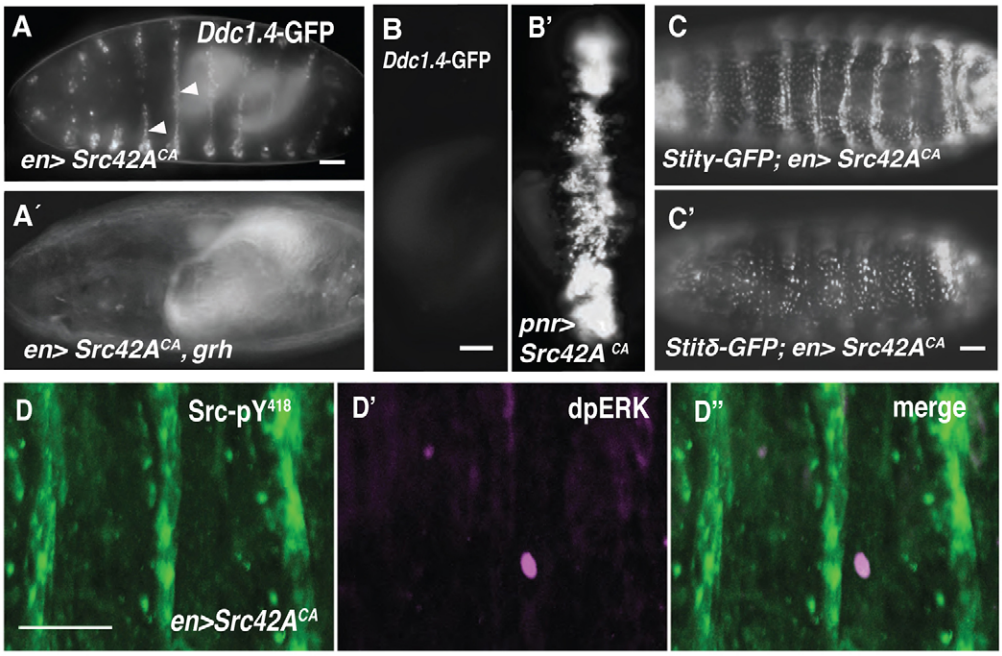

Fig. 7. Grh is required downstream of Src42A for the activation of wound reporters. (A,A′) Ectopic induction of *Ddc1.4*-GFP in engrailed stripes in embryos expressing Src42A^{CA} is marked by arrowheads (A). The striped activation of *Ddc1.4*-GFP is abrogated in *grh*^{37} mutants (A′). (B,B′) Dorsal view of a control embryo at stage 16 expressing the *Ddc1.4*-GFP reporter (B). Ectopic induction of the *Ddc1.4*-GFP reporter in the pannier domain by constitutively active Src42A^{CA} (*pnr*>Src42A^{CA}) (B′). (C,C′) Grh-binding sites are required for the activation of the *Stit*-GFP reporter by *Src42A*. *en*>*Src42A*^{CA} expression causes the ectopic induction of the 2-kb *Stit* γ-GFP reporter (C). The 2-kb *Stit*δ-GFP reporter with mutated Grh-binding sites (C′) cannot be activated by *en*>*Src42A*^{CA} expression. (D–D″) Confocal projections show that dpERK is not ectopically activated by *Src42A*^{CA} in epidermal stripes. Antibody against Src-p^{Y418} detects activated Src (green, D) and antibody against dpERK shows activated ERK (magenta, D′) in *en*>Src42A^{CA} embryos. (D″) shows the overlay of the two channels. Scale bars: 30 μm.

contrast to control embryos, *grh*^{37} mutants expressing Src42A^{CA} in epidermal stripes failed to induce an ectopic GFP signal (Fig. 7A,A′), suggesting that Grh is required downstream of Src42A for *Ddc* activation. Similarly, the *stit*δ reporter, which is identical to *stit*γ but lacks the Grh-binding sites, was not activated by Src42A^{CA} expression (Fig. 7C′). Collectively, these results indicate that Src42A^{CA} induces transcriptional activation of wound reporters by activating Grh. Grh is phosphorylated by ERK, and this modification is necessary for its function following wounding (Kim and McGinnis, 2011). Therefore, we tested the ability of Src42A^{CA} to activate ERK in the embryonic epidermis. Overexpression of either *Src42A*^{CA} or *stit* in epidermal stripes readily activated the *Ddc1.4*-GFP reporter but, in contrast to Stit, Src42A^{CA} failed to induce any detectable dpERK accumulation (Fig. 7D–D″). This suggests that Src activates Grh and the transcription of wound-response genes through an ERK-independent mechanism, presumably involving JNK or other members of the p38 family of kinases (Davis et al., 2008; Sekine et al., 2011; Tateno et al., 2000).

DISCUSSION

Our analysis highlights the crucial role of a single pY in the control of several aspects of wound healing by the Stit RTK. Four effectors bind to pY^{762} to activate multiple parallel intracellular pathways, each controlling distinct aspects of wound healing. Similarly, the SH2 domains of both Grb2 and Src42A bind to the same pY of ErbB (Schulze et al., 2005), suggesting that this method of activating parallel pathways by docking several effectors to the same site is common to several RTKs.

Drk is an adaptor protein with one SH2 and two SH3 domains. In flies, it was first identified and characterized in the context of signaling from the Sevenless receptor tyrosine kinase, where it links the phosphorylated receptor at the plasma membrane (by its SH2 domain) to the Ras guanine-exchange-factor Sos (by its SH3 domain). Ras activation then leads to the activation of a phosphorylation cascade of MAPK kinase (Raf) and Rolled, the *Drosophila* homolog of ERK and MAPK (Biggs et al., 1994; Olivier et al., 1993; Raabe et al., 1995; Simon et al., 1991). Based on our analysis and on previously published work, we propose that the predominant role of Drk in wound healing is to mediate ERK activation and the transcriptional induction of wound-response genes (Fig. 8). In the context of wounding, Stit mutants show reduced dpERK activation, and overexpression of Stit induces ectopic ERK accumulation (Wang et al., 2009). Overexpression of Stit induces dpERK accumulation but embryos expressing Stit^{Y762F}, which does not bind to Drk (or to the other effectors), showed strongly diminished dpERK accumulation. Because the overexpression of the constitutively active version of Src42A can induce the transcriptional activation of wound-response genes without inducing detectable accumulation of dpERK, we suggest that Drk is the major linker between Stit and ERK. ERK phosphorylates Grh *in vitro*, and this phosphorylation is important for the Grh-dependent activation of wound reporters (Kim and McGinnis, 2011). This suggests that the binding of Drk to phosphorylated Stit induces ERK-mediated Grh phosphorylation and *Ddc* activation. Drk might activate an additional pathway downstream of Stit. The SH3 domains of Drk could recruit other downstream effectors, such as Disabled (Le and Simon, 1998) or Cbl (Wang and Pai, 2011), to fulfill the functions of Drk upon Stit activation.

In addition to the anticipated roles of dpERK in gene activation following wounding, we reveal a key function of SFKs in the repair of epidermal injuries. The activation of

Journal of Cell Science (2014) 127, 1829–1839 doi:10.1242/jcs.143016

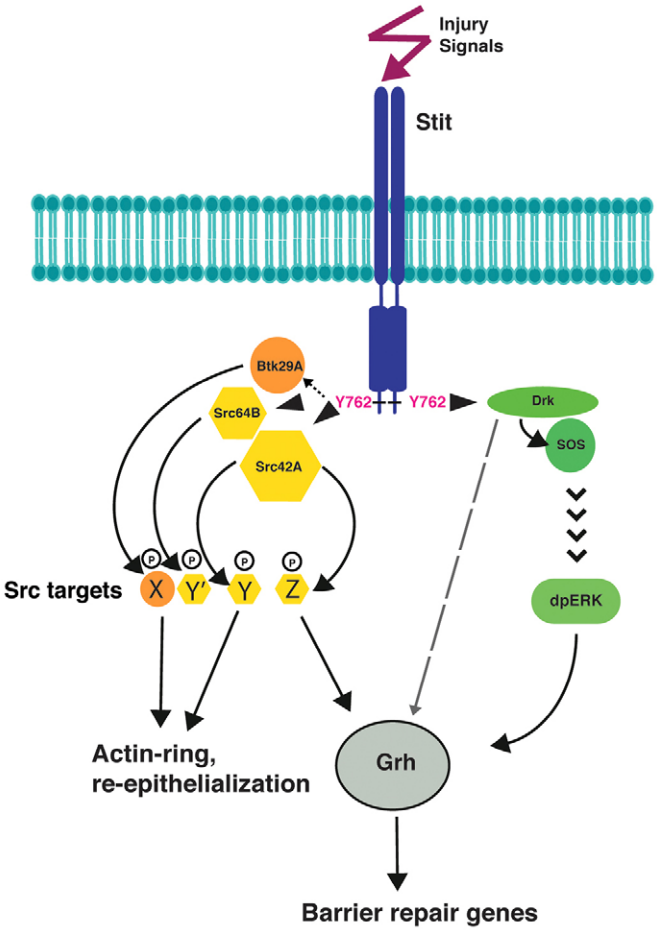

Fig. 8. Model summarizing the proposed functions of Stit effectors during wound healing. Src42A, Src64B and Drk bind to phosphorylated Y762 following wounding and mediate different wound responses. Drk is required for dpERK activation and Grh-dependent transcriptional regulation. Src42 induces both Grh-dependent transcriptional and cytoskeletal responses in parallel to dpERK. Src64B and Btk29A are predominantly involved in cytoskeletal control and re-epithelialization following injury. The model integrates the data from this study and from previously published work.

SFKs has been investigated in several contexts. A standard model involves the de-phosphorylation of Y^{527} of chicken c-src, which unlocks the autoinhibitory interaction and allows trans-auto-phosphorylation (Yeatman, 2004). More recently, cysteine oxidation by reactive oxygen species has emerged as a mechanism for Src activation in epithelial cells and leukocytes during wound healing in zebrafish (Yoo et al., 2012). Our results reveal an additional RTK-dependent mechanism for the immediate SFK activation at the wound site. Phosphorylation of Y^{762} of Stit might provide a high-affinity binding site for the SH2 domain of Src kinases, which would therefore compete with the autoinhibitory interaction of the SH2 domain with Y^{511} in Src42A. This would lead to full activation either by autophosphorylation or by trans-phosphorylation by Stit (Fig. 8). This is the mechanism by which Src is recruited to and activated on the docking site of the PDGF receptor in porcine aortic endothelial cells (Mori et al., 1993).

Following wounding or Stit activation, SFKs control both the local induction of wound-response genes by the conserved transcription factor Grh, and the assembly of a distinctive actin cable around the wound edge. Interestingly, Src42A is the predominant player in transcriptional activation. During late embryonic development, Src42A restricts *Ddc* expression in epidermal cells. However, following injury, it is required for the local induction of *Ddc*. Additionally, $Src42A^{CA}$ can ectopically activate wound-response genes without causing any detectable accumulation of dpERK. This suggests a novel dpERK-independent mechanism of Grh activation during wound healing. Our results contrast with the observations of Juarez and colleagues (Juarez et al., 2011), who reported that injury of *src42A* mutant embryos results in widespread activation of wound-response genes along the entire epidermis. There are several explanations for this discrepancy. First, Juarez et al. (Juarez et al., 2011), recorded the GFP intensity of *Ddc*.47, a minimal wound enhancer reporter presumably lacking the cis-elements that drive the developmental expression of *Ddc* in the epidermis and other tissues (Mace et al., 2005). Second, the widespread activation of *Ddc*.47 was recorded several hours after the interval of our assays. Thus, our analysis reveals the immediate role of Src42A in the activation of wound-response genes at the injury site, whereas the results of Juarez et al. (Juarez et al., 2011) might suggest a later, direct or indirect, role of Src42A in restricting the spread of the response. The different mechanisms of Src activation by phosphorylation or cysteine oxidation might provide a clue as to how Src42A can act both as a repressor of epidermal *Ddc* expression during development and as an activator of *Ddc* and other genes upon injury. Basal low levels of Src42A phosphorylation in the epidermis might favor *Ddc* repression, whereas increased levels of p-Src by Stit or other RTKs following injury might lead to the Grh-dependent activation of wound-response genes.

We found that re-epithelialization after injury is controlled by all three non-RTKs, because double mutants show more pronounced defects in wound closure than single $src42A^{E1}$ mutants. The assembly of the actin ring requires the coordination of the cytoskeleton across the membranes of the epithelial cells surrounding the wound edge. Because Src42A has been implicated in the control of E-cadherin trafficking, it is tempting to speculate that its role in re-epithelialization is to control the adhesion of the leading cells, thereby controlling wound constriction (Abreu-Blanco et al., 2012; Förster and Luschnig, 2012; Nelson et al., 2012). By contrast, Btk29A and Src64B control the growth of the actin-rich ovarian ring canals (Lu et al., 2004) and microfilament contraction during cellularization (Thomas and Wieschaus, 2004), suggesting that they might preferentially control actin-filament assembly and contraction at the wound edge. Besides Stit and its effectors, the Rho GTPase and profilin and Karst (a *Drosophila* β-heavy spectrin homolog) have also been shown to participate in the formation of a continuous actin cable (Brock et al., 2012; Campos et al., 2010; Wood et al., 2002), suggesting that they might represent downstream targets of Src and Btk29A during re-epithelialization. Our analysis reveals distinct roles for RTK effectors in wound-healing responses, and provides a molecular framework towards understanding and manipulating RTK signaling during wound healing.

MATERIALS AND METHODS

Fly genetics and transgenic lines

Crosses were performed at 25°C on standard medium unless indicated otherwise. The w^{1118} strain was used as the wild-type control. We expressed the actin-binding domain of Moesin fused to GFP under the control of the *sqh* (myosin II regulatory light chain) promoter (sGMCA) (Kiehart et al., 2000) to examine both epithelial repair and actin-cable

assembly after wounding. The UAS-*stit*^{Y751F} and UAS-*stit*^{Y762F} strains were generated by cloning the mutated *stit* versions into the pUAST vector, followed by standard P-element-mediated transformation. The mutant alleles used were: *src42A*^{E1}, *src64B*, *drk*^{eOA}, *btk*^{k206} and *grh*^{B37}. *en*-GAL4 (Bloomington Stock Center) and *pnr*-GAL4 (Calleja et al., 2000) were used to drive UAS-*Src42A*^{CA} (Kyoto Stock Center). The 2-kb *stitγ*-GFP, 2-kb *stitδ*-GFP, UAS-*stit*, UAS-*stit*^{K504A}, UAS-*stit*^{Y751F} and UAS-*stit*^{Y762F} were expressed in epidermal stripes at 25℃. The 1.4-kb *Ddc1.4*-GFP and the 3.0-kb *ple*-DsRed wound reporters (Mace et al., 2005) were used to assess *Ddc* and *Ple* induction following wounding. In the *stit*-lethality rescue experiment, the UAS-*stit*, UAS-*stit*^{K504A} and UAS-*stit*^{Y762F} transgenes were expressed in *stit* mutant embryos under the control of the epithelial driver *69B*-GAL4. *Dfd*-GFP-marked CyO and TM3 (or TM6) balancers were used to identify homozygous mutant embryos.

Yeast two-hybrid screen

The screen was carried out by Hybrigenics using a prey library constructed from RNA from embryos that were 0–24-h old. A fragment encoding the intracellular domain of Stit (amino acids 337–773) was inserted into the pB27 vector (N-Lex–bait-C fusion) and was used to screen 72.7 million clones. 185 positive clones were sequenced and classified according to the interaction confidence by Hybrigenics.

Immunohistochemistry and *in situ* hybridization

Immunohistochemistry was performed as described previously (Hemphälä et al., 2003). We used the following primary antibodies: rabbit polyclonal anti-Src (phospho-Y418, 1:500, Invitrogen), guinea-pig anti-Stit (1:500, Wang et al., 2009), mouse anti-diphosphorylated ERK (dpERK) (1:100, Sigma), mouse anti-phosphotyrosine (pY) (1:100, Upstate Cell Signaling), mouse anti-GFP (1:400, Sigma). Secondary antibodies conjugated to Cy2, Cy3 (Jackson Immunochemicals) or Alexa Fluor 488 (Molecular Probes) were used at 1:400. Whole-mount RNA *in situ* hybridization using digoxigenin-labeled probes was conducted as described previously (Lehmann and Tautz, 1994). Heterozygous mutant embryos carrying the LacZ balancer were distinguished from homozygous mutant embryos by staining with rabbit anti-β-gal primary antibody (1:1000, Cappel).

Cell culture, GST pull-down and western blotting

PCR fragments comprising the full-length of Stit, Stit^{K504A}, Stit^{Y553F}, Stit^{Y572F}, Stit^{Y660F}, Stit^{Y717F}, Stit^{Y751F}, Stit^{Y762F} and Stit$^{Y751F/Y762F}$ were sub-cloned in frame with a C-terminal V5 tag into pMT expression vector (Invitrogen), and transfected into *Drosophila* S2 cells using the Effectene kit (Qiagen). At 72 h after transfection, cells were harvested in 125 mM pyrophosphate, 1 M sodium fluoride, 1 M β-glycerophosphate and 500 mM sodium orthovanadate. PCR fragments comprising the sequences coding for the SH2 domain of Drk, Src42A and Src64B were sub-cloned into the pGEX-4T-1 vector.

Expression of the GST–Drk fusion protein and GST–Src64 fusion protein in *Escherichia coli* BL21 cells were induced with isopropyl-β-D-thiogalactopyranoside (IPTG) for 2 h at 25℃. Expression of the GST–Src-42 fusion protein in *E. coli* BL21 cells was induced with IPTG for 2.4 h at 25℃, followed by purification on glutathione–Sepharose beads (GE Healthcare). The beads were washed three times in GST lysis buffer (20 mM Tris-HCl pH 8.0, 200 mM NaCl, 1 mM EDTA, 0.1% NP-40). AEBSF [4-(2-aminoethyl) benzenesulfonyl fluoride hydrochloride] (Sigma) and complete protease inhibitor cocktail tablets (Roche) were added to the GST lysis buffer before use. Proteins bound to the beads were eluted by addition of GSH buffer (20 mM glutathione, 50 mM Tris-HCl pH 8.0) and were analyzed by SDS-PAGE (10% SDS) followed by exposure to an FLA 1000 phosphorimager (Fuji). The following antibodies were used at the indicated dilutions: anti-GST (1:2500, Santa Cruz), anti-V5 (1:5000, Invitrogen).

Embryo wounding

Embryos were collected during early stage 15 (11 h after egg laying at 25℃), were dechorionated in bleach and placed on a gas-permeable membrane stretched over two silicon bars on a slide (Tsarouhas et al., 2007). Embryos were mounted in halocarbon 700 oil and covered with a cover glass (Menzel-Gläser). Embryos were wounded on the ventral side using a nitrogen pulsed laser (VSL-337ND-S; Laser Science) tuned to 440 nm. The laser was connected to an upright microscope (Axioplan2; Zeiss) equipped with a ×63/1.2NA C-Apochromat water-immersion objective (Zeiss). Ablations were monitored by using the MicroPoint Ablation System (Andor Technologies). Our laser-wounding procedure resulted in mean wound sizes of 1147.29 μm^2 (±98.37) and 1197.21 μm^2 (±83.95) (mean±s.e.m.) in wild-type and mutant embryos, respectively.

Embryos carrying the *Ddc1.4*-GFP or the *Ple*-DsRed reporters were puncture-wounded with a sterile injection capillary as described previously (Mace et al., 2005). Pricked embryos covered with halocarbon 700 oil were allowed to develop for 3 h before imaging. The extent of GFP or DsRed induction at the wound edge was classified as strong, moderate or weak by two independent observers.

Live imaging

Live imaging using wide-field fluorescence microscopy was performed to estimate the time taken for wound closure as described previously (Wang et al., 2009). Wounded wild-type and mutant embryos were placed on the same slide and imaged in parallel. Confocal live imaging was used to examine the actin cytoskeleton during re-epithelialization. Laser-wounded embryos were transferred to a laser-scanning confocal microscope (LSM 510 META or LSM780; Zeiss) and imaged with an Argon 2 488-nm laser using a ×63/1.3NA C-Apochromat water-immersion objective (Zeiss). Individual *z*-stacks with a step size of 1–2.5 μm were taken every 6 min over a 3–8-h period. Recording was initiated approximately 30 min after wounding. All recorded embryos developed to late stage 17. Time-lapse movies were created from confocal *z*-stack projections (maximum intensity) by using NIH ImageJ software from http://rsb.info.nih.gov/ij/index.html.

Quantification of GFP–Moesin fluorescence intensity

Semi-quantitative analysis of the fluorescence intensity of GFP–Moesin during re-epithelialization was performed essentially as described previously (Wang et al., 2009). Confocal *z*-stacks, 22–30 μm in total thickness, were collected to cover the entire puncture depth of the epidermis. Intensities were estimated from the sum of signals of the *z*-stack. RFI at the wound edge (Bement et al., 1993) was calculated from projected stack images at defined time-points in each embryo by using the formula RFI=*FI*w/*FI*ep, where *FI*w represents the average intensity within the area of a 1.2-μm ring around the wound edge and *FI*ep represents the average intensity in a concentric ring area located at a distance of 8 μm from the wound border. Mean RFI values were calculated for each time-point and were plotted in the graph shown in Fig. 5E. The time-points in wild-type embryos represent the start, quarter, half and three quarters of the mean closure time and the final closure time. *src42A*^{E1}, *src42A*^{E1} *btk29A* and *src42A*^{E1} *src64B* mutant embryos required more time to close their wounds, or failed wound closure. Therefore, two time-points were added in experiments with these embryos – one at the mean of *src42A*^{E1} wound-closure time and one at the final recording time. The *xy* projections and the quantification of fluorescence intensity measurements were performed in ImageJ.

Statistics

Error bars in all graphs indicate s.e.m. An unpaired two-tailed Student's *t*-test was used to estimate statistical significance, unless indicated.

Acknowledgements

We are indebted to Naumi Nautiyal, who initiated the analysis of Stit effectors and performed several of the experiments. We would like to thank members of our laboratory and Mattias Mannervik (Stockholm University, Stockholm, Sweden) for support, discussions and critical reading of the manuscript. We thank Monika Björk for help with the generation of transgenic strains. We thank William McGinnis (University of California at San Diego, San Diego, CA) for wound reporters, Bloomington and Kyoto Stock Centers for fly strains, and the imaging facility at Stockholm University (IFSU). The two-hybrid screen was carried out by Hybrigenics.

Competing interests

The authors declare no competing interests.

Author contributions

V. T., L. Y. and C. S. planned the experiments. V. T. generated and analyzed strains by live imaging and confocal microscopy. L. Y. performed the protein-binding assays, and generated and analyzed mutant strains. C. S. analyzed the data and wrote the manuscript together with V. T. and L.Y.

Funding

This work was supported by grants from the Swedish Research Council VR-M [grant number K2010-67X-21476-01-3]; and Cancerfonden [grant number 1245222].

Supplementary material

Supplementary material available online at
http://jcs.biologists.org/lookup/suppl/doi:10.1242/jcs.143016/-/DC1

References

Abreu-Blanco, M. T., Verboon, J. M., Liu, R., Watts, J. J. and Parkhurst, S. M. (2012). Drosophila embryos close epithelial wounds using a combination of cellular protrusions and an actomyosin purse string. *J. Cell Sci.* **125**, 5984-5997.

Bement, W. M., Forscher, P. and Mooseker, M. S. (1993). A novel cytoskeletal structure involved in purse string wound closure and cell polarity maintenance. *J. Cell Biol.* **121**, 565-578.

Biggs, W. H., 3rd, Zavitz, K. H., Dickson, B., van der Straten, A., Brunner, D., Hafen, E. and Zipursky, S. L. (1994). The Drosophila rolled locus encodes a MAP kinase required in the sevenless signal transduction pathway. *EMBO J.* **13**, 1628-1635.

Brock, A. R., Wang, Y., Berger, S., Renkawitz-Pohl, R., Han, V. C., Wu, Y. and Galko, M. J. (2012). Transcriptional regulation of Profilin during wound closure in Drosophila larvae. *J. Cell Sci.* **125**, 5667-5676.

Calleja, M., Herranz, H., Estella, C., Casal, J., Lawrence, P., Simpson, P. and Morata, G. (2000). Generation of medial and lateral dorsal body domains by the pannier gene of Drosophila. *Development* **127**, 3971-3980.

Campos, I., Geiger, J. A., Santos, A. C., Carlos, V. and Jacinto, A. (2010). Genetic screen in Drosophila melanogaster uncovers a novel set of genes required for embryonic epithelial repair. *Genetics* **184**, 129-140.

Chmielowiec, J., Borowiak, M., Morkel, M., Stradal, T., Munz, B., Werner, S., Wehland, J., Birchmeier, C. and Birchmeier, W. (2007). c-Met is essential for wound healing in the skin. *J. Cell Biol.* **177**, 151-162.

Davis, M. M., Primrose, D. A. and Hodgetts, R. B. (2008). A member of the p38 mitogen-activated protein kinase family is responsible for transcriptional induction of Dopa decarboxylase in the epidermis of Drosophila melanogaster during the innate immune response. *Mol. Cell. Biol.* **28**, 4883-4895.

Förster, D. and Luschnig, S. (2012). Src42A-dependent polarized cell shape changes mediate epithelial tube elongation in Drosophila. *Nat. Cell Biol.* **14**, 526-534.

Gabay, L., Seger, R. and Shilo, B. Z. (1997). MAP kinase in situ activation atlas during Drosophila embryogenesis. *Development* **124**, 3535-3541.

Galko, M. J. and Krasnow, M. A. (2004). Cellular and genetic analysis of wound healing in Drosophila larvae. *PLoS Biol.* **2**, e239.

Geiger, J. A., Carvalho, L., Campos, I., Santos, A. C. and Jacinto, A. (2011). Hole-in-one mutant phenotypes link EGFR/ERK signaling to epithelial tissue repair in Drosophila. *PLoS ONE* **6**, e28349.

Gurtner, G. C., Werner, S., Barrandon, Y. and Longaker, M. T. (2008). Wound repair and regeneration. *Nature* **453**, 314-321.

Hemphälä, J., Uv, A., Cantera, R., Bray, S. and Samakovlis, C. (2003). Grainy head controls apical membrane growth and tube elongation in response to Branchless/FGF signalling. *Development* **130**, 249-258.

Juarez, M. T., Patterson, R. A., Sandoval-Guillen, E. and McGinnis, W. (2011). Duox, Flotillin-2, and Src42A are required to activate or delimit the spread of the transcriptional response to epidermal wounds in Drosophila. *PLoS Genet.* **7**, e1002424.

Kiehart, D. P., Galbraith, C. G., Edwards, K. A., Rickoll, W. L. and Montague, R. A. (2000). Multiple forces contribute to cell sheet morphogenesis for dorsal closure in Drosophila. *J. Cell Biol.* **149**, 471-490.

Kim, M. and McGinnis, W. (2011). Phosphorylation of Grainy head by ERK is essential for wound-dependent regeneration but not for development of an epidermal barrier. *Proc. Natl. Acad. Sci. USA* **108**, 650-655.

Laberge, G., Douziech, M. and Therrien, M. (2005). Src42 binding activity regulates Drosophila RAF by a novel CNK-dependent derepression mechanism. *EMBO J.* **24**, 487-498.

Le, N. and Simon, M. A. (1998). Disabled is a putative adaptor protein that functions during signaling by the sevenless receptor tyrosine kinase. *Mol. Cell. Biol.* **18**, 4844-4854.

Lehmann, R. and Tautz, D. (1994). In situ hybridization to RNA. *Methods Cell Biol.* **44**, 575-598.

Lemmon, M. A. and Schlessinger, J. (2010). Cell signaling by receptor tyrosine kinases. *Cell* **141**, 1117-1134.

Lesch, C., Jo, J., Wu, Y., Fish, G. S. and Galko, M. J. (2010). A targeted UAS-RNAi screen in Drosophila larvae identifies wound closure genes regulating distinct cellular processes. *Genetics* **186**, 943-957.

Lu, N., Guarnieri, D. J. and Simon, M. A. (2004). Localization of Tec29 to ring canals is mediated by Src64 and PtdIns(3,4,5)P3-dependent mechanisms. *EMBO J.* **23**, 1089-1100.

Mace, K. A., Pearson, J. C. and McGinnis, W. (2005). An epidermal barrier wound repair pathway in Drosophila is mediated by grainy head. *Science* **308**, 381-385.

Meyer, M., Müller, A. K., Yang, J., Moik, D., Ponzio, G., Ornitz, D. M., Grose, R. and Werner, S. (2012). FGF receptors 1 and 2 are key regulators of keratinocyte migration in vitro and in wounded skin. *J. Cell Sci.* **125**, 5690-5701.

Mori, S., Rönnstrand, L., Yokote, K., Engström, A., Courtneidge, S. A., Claesson-Welsh, L. and Heldin, C. H. (1993). Identification of two juxtamembrane autophosphorylation sites in the PDGF beta-receptor; involvement in the interaction with Src family tyrosine kinases. *EMBO J.* **12**, 2257-2264.

Müller, A. K., Meyer, M. and Werner, S. (2012). The roles of receptor tyrosine kinases and their ligands in the wound repair process. *Semin. Cell Dev. Biol.* **23**, 963-970.

Nada, S., Okada, M., MacAuley, A., Cooper, J. A. and Nakagawa, H. (1991). Cloning of a complementary DNA for a protein-tyrosine kinase that specifically phosphorylates a negative regulatory site of p60c-src. *Nature* **351**, 69-72.

Nelson, K. S., Khan, Z., Molnár, I., Mihály, J., Kaschube, M. and Beitel, G. J. (2012). Drosophila Src regulates anisotropic apical surface growth to control epithelial tube size. *Nat. Cell Biol.* **14**, 518-525.

Olivier, J. P., Raabe, T., Henkemeyer, M., Dickson, B., Mbamalu, G., Margolis, B., Schlessinger, J., Hafen, E. and Pawson, T. (1993). A Drosophila SH2-SH3 adaptor protein implicated in coupling the sevenless tyrosine kinase to an activator of Ras guanine nucleotide exchange, Sos. *Cell* **73**, 179-191.

Pearson, J. C., Juarez, M. T., Kim, M., Drivenes, Ø. and McGinnis, W. (2009). Multiple transcription factor codes activate epidermal wound-response genes in Drosophila. *Proc. Natl. Acad. Sci. USA* **106**, 2224-2229.

Raabe, T., Olivier, J. P., Dickson, B., Liu, X., Gish, G. D., Pawson, T. and Hafen, E. (1995). Biochemical and genetic analysis of the Drk SH2/SH3 adaptor protein of Drosophila. *EMBO J.* **14**, 2509-2518.

Rämet, M., Lanot, R., Zachary, D. and Manfruelli, P. (2002). JNK signaling pathway is required for efficient wound healing in Drosophila. *Dev. Biol.* **241**, 145-156.

Razzell, W., Wood, W. and Martin, P. (2011). Swatting flies: modelling wound healing and inflammation in Drosophila. *Dis. Model. Mech.* **4**, 569-574.

Razzell, W., Evans, I. R., Martin, P. and Wood, W. (2013). Calcium flashes orchestrate the wound inflammatory response through DUOX activation and hydrogen peroxide release. *Curr. Biol.* **23**, 424-429.

Sadowski, I., Stone, J. C. and Pawson, T. (1986). A noncatalytic domain conserved among cytoplasmic protein-tyrosine kinases modifies the kinase function and transforming activity of Fujinami sarcoma virus P130gag-fps. *Mol. Cell. Biol.* **6**, 4396-4408.

Schulze, W. X., Deng, L. and Mann, M. (2005). Phosphotyrosine interactome of the ErbB-receptor kinase family. *Mol. Syst. Biol.* **1**, 2005 0008.

Sekine, Y., Takagahara, S., Hatanaka, R., Watanabe, T., Oguchi, H., Noguchi, T., Naguro, I., Kobayashi, K., Tsunoda, M., Funatsu, T. et al. (2011). p38 MAPKs regulate the expression of genes in the dopamine synthesis pathway through phosphorylation of NR4A nuclear receptors. *J. Cell Sci.* **124**, 3006-3016.

Shindo, M., Wada, H., Kaido, M., Tateno, M., Aigaki, T., Tsuda, L. and Hayashi, S. (2008). Dual function of Src in the maintenance of adherens junctions during tracheal epithelial morphogenesis. *Development* **135**, 1355-1364.

Simon, M. A., Bowtell, D. D., Dodson, G. S., Laverty, T. R. and Rubin, G. M. (1991). Ras1 and a putative guanine nucleotide exchange factor perform crucial steps in signaling by the sevenless protein tyrosine kinase. *Cell* **67**, 701-716.

Takahashi, F., Endo, S., Kojima, T. and Saigo, K. (1996). Regulation of cell-cell contacts in developing Drosophila eyes by Dsrc41, a new, close relative of vertebrate c-src. *Genes Dev.* **10**, 1645-1656.

Tateno, M., Nishida, Y. and Adachi-Yamada, T. (2000). Regulation of JNK by Src during Drosophila development. *Science* **287**, 324-327.

Thomas, J. H. and Wieschaus, E. (2004). src64 and tec29 are required for microfilament contraction during Drosophila cellularization. *Development* **131**, 863-871.

Ting, S. B., Caddy, J., Hislop, N., Wilanowski, T., Auden, A., Zhao, L. L., Ellis, S., Kaur, P., Uchida, Y., Holleran, W. M. et al. (2005). A homolog of Drosophila grainy head is essential for epidermal integrity in mice. *Science* **308**, 411-413.

Tsarouhas, V., Senti, K. A., Jayaram, S. A., Tiklová, K., Hemphälä, J., Adler, J. and Samakovlis, C. (2007). Sequential pulses of apical epithelial secretion and endocytosis drive airway maturation in Drosophila. *Dev. Cell* **13**, 214-225.

Vidal, M., Warner, S., Read, R. and Cagan, R. L. (2007). Differing Src signaling levels have distinct outcomes in Drosophila. *Cancer Res.* **67**, 10278-10285.

Wang, P. Y. and Pai, L. M. (2011). D-Cbl binding to Drk leads to dose-dependent down-regulation of EGFR signaling and increases receptor-ligand endocytosis. *PLoS ONE* **6**, e17097.

Wang, S. and Samakovlis, C. (2012). Grainy head and its target genes in epithelial morphogenesis and wound healing. *Curr. Top. Dev. Biol.* **98**, 35-63.

Wang, S., Tsarouhas, V., Xylourgidis, N., Sabri, N., Tiklová, K., Nautiyal, N., Gallio, M. and Samakovlis, C. (2009). The tyrosine kinase Stitcher activates Grainy head and epidermal wound healing in Drosophila. *Nat. Cell Biol.* **11**, 890-895.

Wood, W., Jacinto, A., Grose, R., Woolner, S., Gale, J., Wilson, C. and Martin, P. (2002). Wound healing recapitulates morphogenesis in Drosophila embryos. *Nat. Cell Biol.* **4**, 907-912.

Wood, W., Faria, C. and Jacinto, A. (2006). Distinct mechanisms regulate hemocyte chemotaxis during development and wound healing in Drosophila melanogaster. *J. Cell Biol.* **173**, 405-416.

Wouda, R. R., Bansraj, M. R., de Jong, A. W., Noordermeer, J. N. and Fradkin, L. G. (2008). Src family kinases are required for WNT5 signaling through the Derailed/RYK receptor in the Drosophila embryonic central nervous system. *Development* **135**, 2277-2287.

Yeatman, T. J. (2004). A renaissance for SRC. *Nat. Rev. Cancer* **4**, 470-480.

Yoo, S. K., Freisinger, C. M., LeBert, D. C. and Huttenlocher, A. (2012). Early redox, Src family kinase, and calcium signaling integrate wound responses and tissue regeneration in zebrafish. *J. Cell Biol.* **199**, 225-234.

A

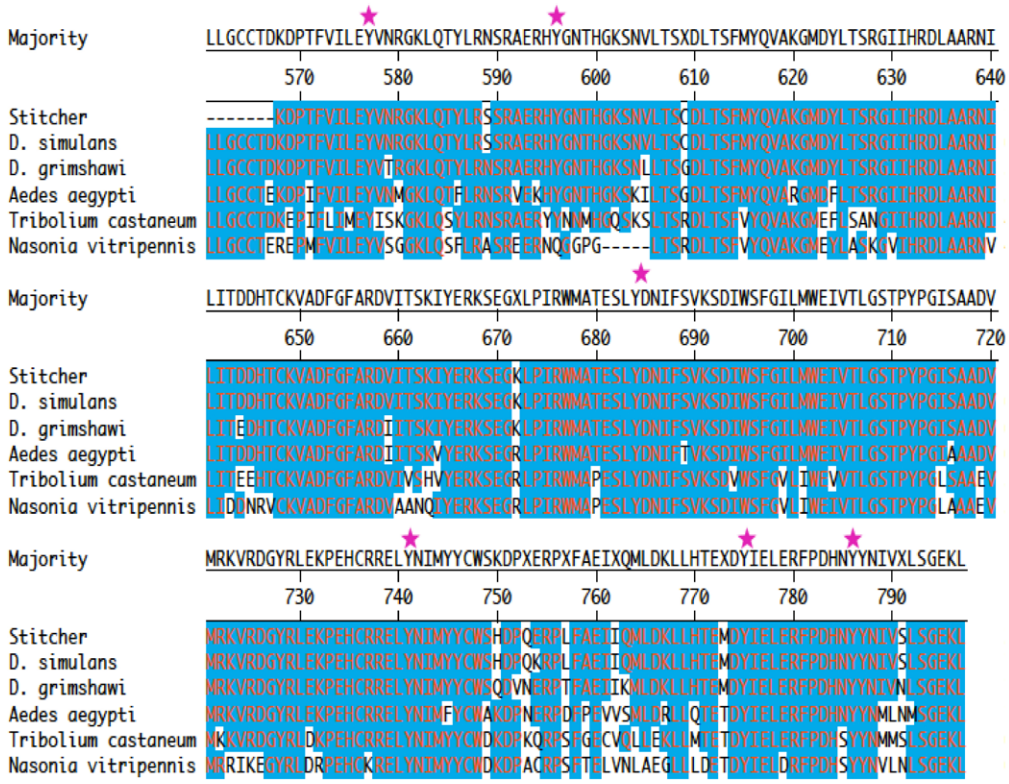

B

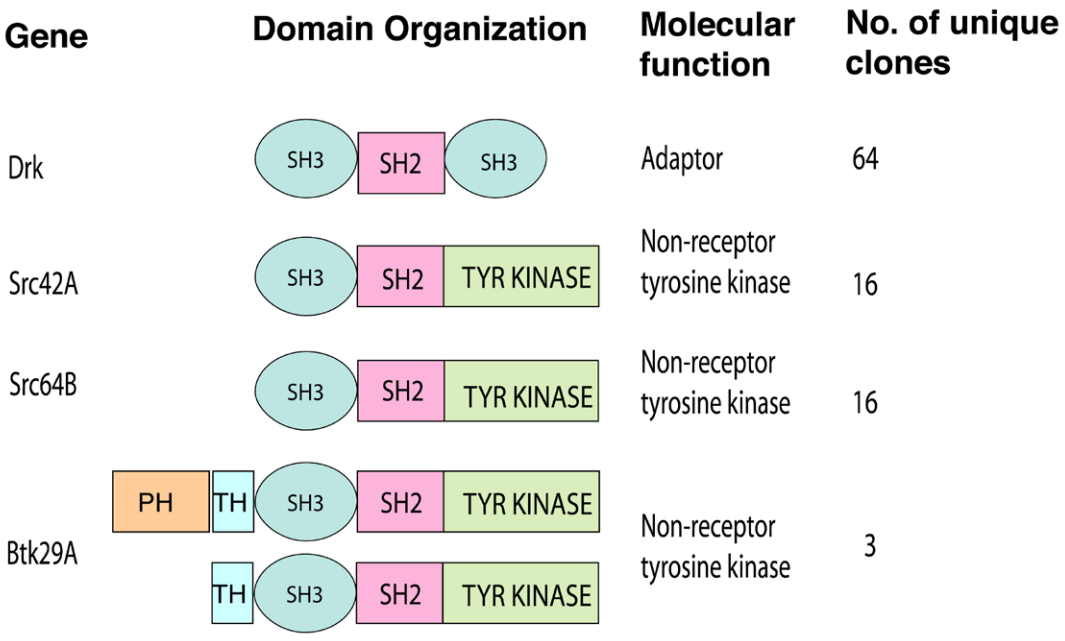

Fig. S1. Stit conservation across phylogeny. (A) Multiple alignment of intracellular domains of Stitcher identifying conserved tyrosines. Tyrosines targeted for analysis have been marked with a red asterisk. Significant conservation is observed from other insects up to higher vertebrates. (B) A schematic illustration of the Yeast two-hybrid screen results, depicting the domain organization of each interacting partner and the positive number of clones.

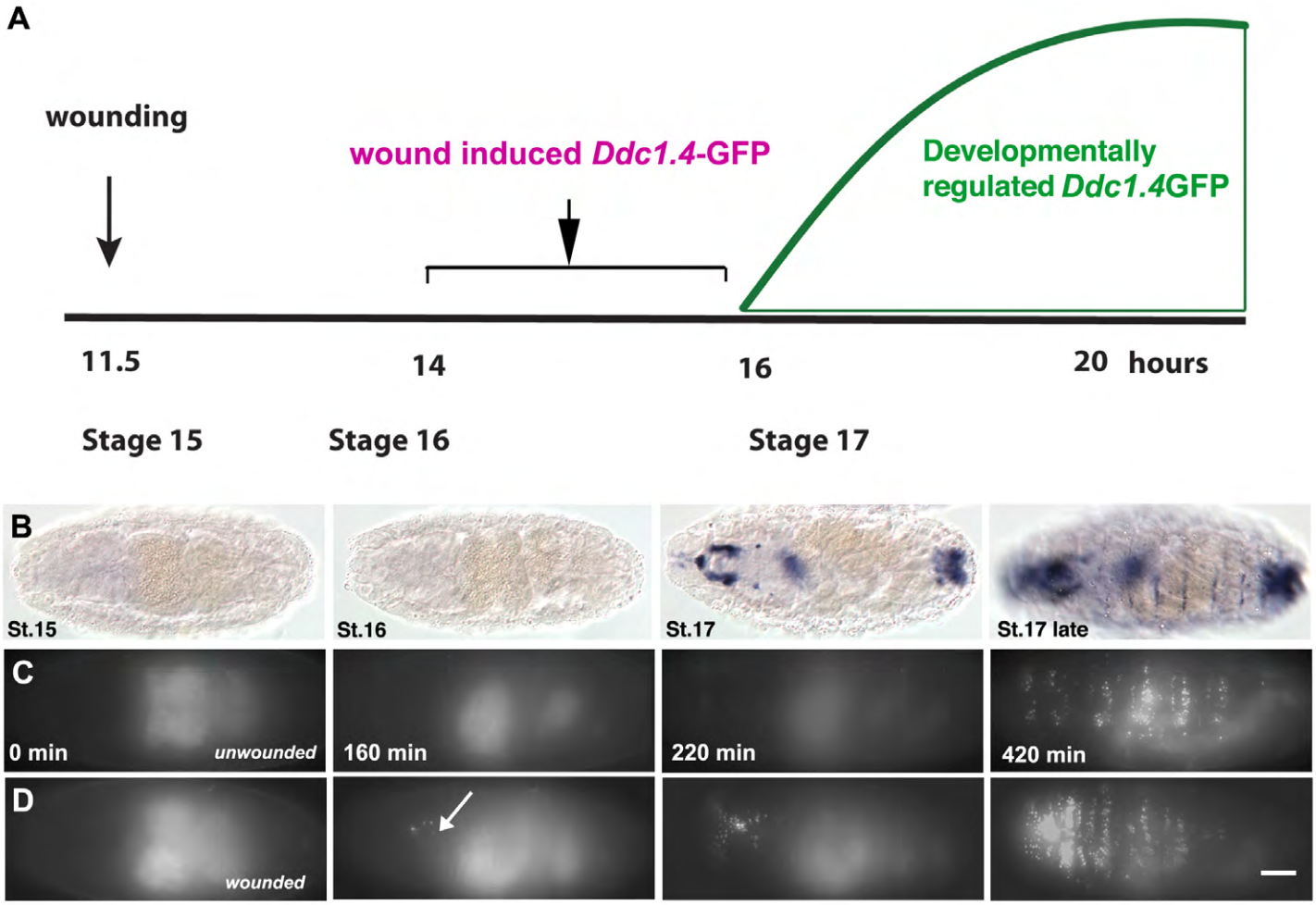

Fig. S2. Induction of *Ddc1.4*-GFP reporter during embryonic development. (A) Graphical illustration of the developmental *Ddc1.4*-GFP induction in wild-type embryos. Developmental *Ddc1.4*-GFP induction occurs at stage 17. In order to avoid the interference of the developmental activation of *Ddc1.4*-GFP reporter, we performed wounding at 11.5 hours of embryonic development (stage 15) and we assessed wound induced *Ddc1.4*-GFP at 14–16 hours of embryonic development (stage 16) before *Ddc1.4*-GFP induced developmentally. (B). *In situ* hybridization with an antisense *Ddc* probe in wild-type unwounded embryos. *Ddc* transcript is accumulated at late stage 17. (C,D) Projections of time-lapse images showing *Ddc1.4*-GFP induction in an unwounded (C) and a wounded wild-type embryo (D) expressing the *Ddc1.4*-GFP reporter. Arrow indicates the site of wounding. Embryos were imaged in parallel and recording times are indicated. Scale bar, 50 μm.

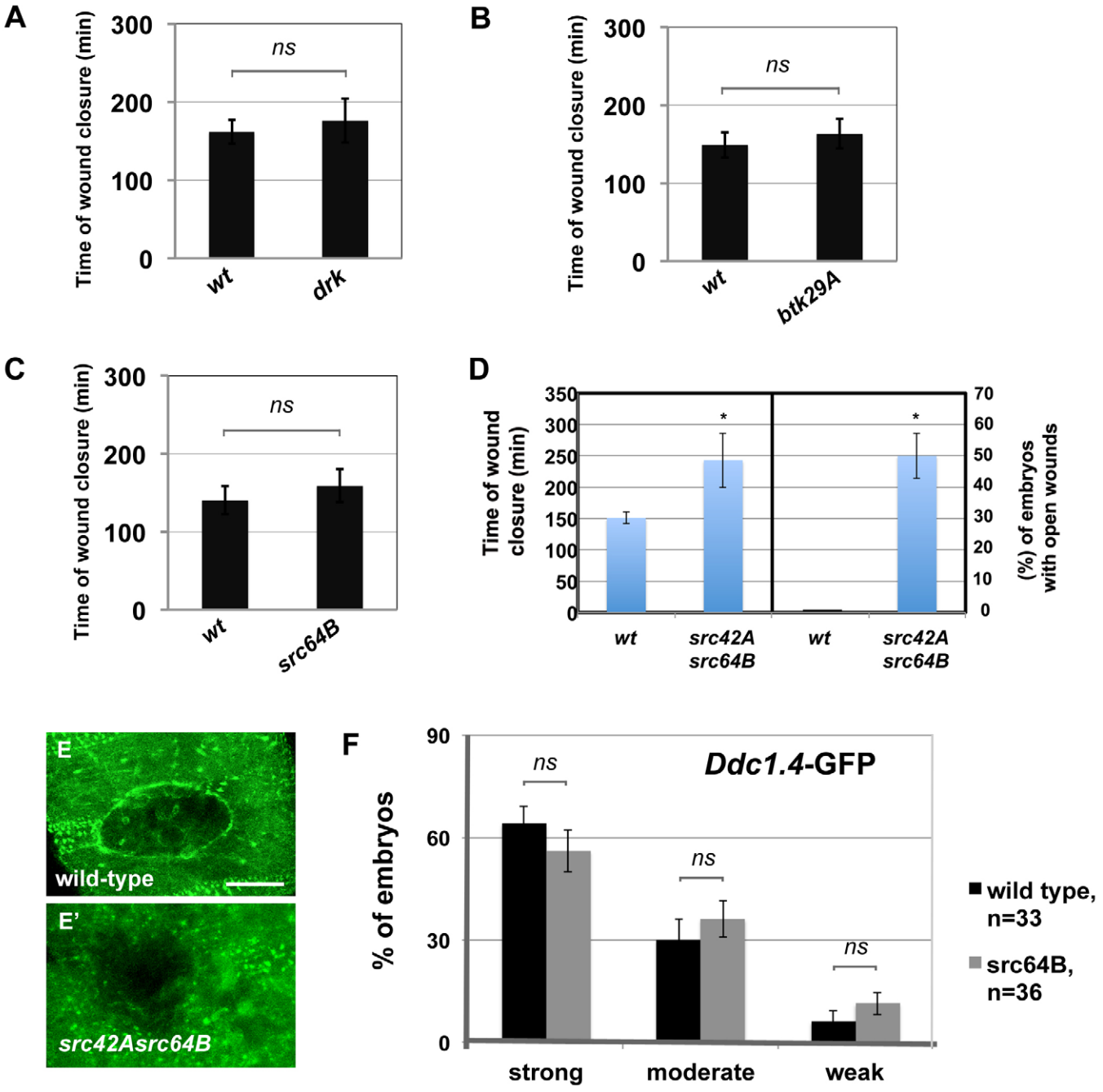

Fig. S3. Re-epithelialization after wounding in *drk*, *src42Asrc64B*, *btk29A* and *src64B* mutant embryos. Wound induction of *Ddc1.4*-GFP reporter in *src64B* mutants. (A-D) Bar graphs showing the average time of wound closure in wounded *drk* (A), *btk29A* (B), *src64B* (C) and *src42Asrc64B* (D) mutant embryos expressing *sqh*-GFPmoe. Single *drk* (*n=13*), *btk29A* (*n=18*) and *src64B* (*n=20*) mutants showed no differences in the average time of wound closure as compared to the control (wild-types). *src42Asrc64B* (*n=14*) double mutant showed a significant delay in re-epithelialization after wounding and only 50% of the embryos closed their wounds (D). *ns* and * denote, $P>0.05$ and $P<0.001$ respectively. E-E′. Confocal projections of epidermal wounds in a wild-type (E) and a *src42Asrc64B* (E′) mutant embryo expressing *sqh*-GFPmoe. The actin cable around the wound edge is absent in the double *src42Asrc64B* mutant. Scale bar, 20 µm. (F) Quantification of the *Ddc1.4*-GFP reporter induction in wounded control (*n=33*) and *src64B* (*n=36*) mutant embryos. *Ddc1.4*-GFP expression classified as strong, moderate and weak based on the extent of GFP signals at the wounding site. The *y*-axis shows the percentage (%) of embryos that show the phenotype. The mean (±s.e.m) of three independent experiments is shown. *ns* denotes, $P>0.05$.

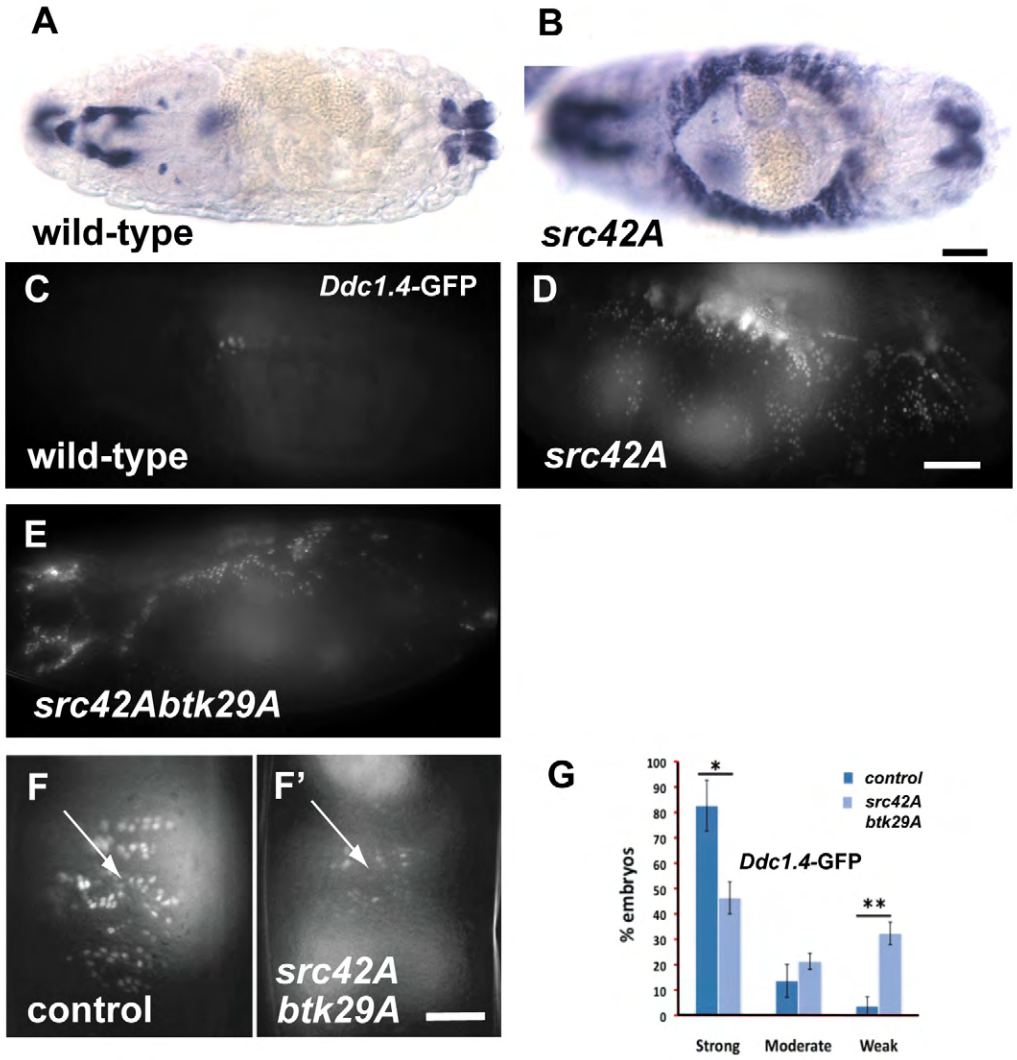

Fig. S4. Developmental induction of *Ddc* in *src42A* and *src42Abtk29A* mutant embryos. Src42A is required for wound reporter activation upon injury. (A–B) *In situ* hybridization with an antisense *Ddc* probe in wild-type (A) and *src42A* (B) unwounded embryos at late stage 16. *src42A* mutant embryos show dorsal closure phenotype and a predominant *Ddc* expression in the dorsal hole region (B). (C-E) Images from time-lapse recordings showing an unwounded wild-type (C), src42A (D) and a *src42Abtk29A* mutant (D) embryo expressing the *Ddc1.4*-GFP reporter. *src42A* and *src42Abtk29A* mutant embryos show strong *Ddc1.4*-GFP expression in dorsal epidermis. (F-F′) *Ddc1.4*-GFP reporter induction after wounding is reduced in *src42Abtk29A* (F′) double mutants, as compared to control embryos (wild-type, *Ddc1.4*-GFP) (F). Induction was imaged 3 hours post-wounding. Arrows mark the wound entry site. (G) Quantification of *Ddc1.4*-GFP reporter induction in wounded control (wild-type, *n=86*) and in *src42Abtk29A* double mutants (*n=86*). *Ddc1.4*-GFP induction classified as strong, moderate and weak based on the extent of GFP signal at the wounds. The *y*-axis shows percentage of wounded embryos that show each phenotypic category. The mean of three independent experiments (±s.e.m) is shown. * and ** denote $P<0.05$ and $P<0.01$ respectively. Scale bars, 50 µm

Supplementary Movie 1. Time-lapse movie showing the *Ddc1.4*-GFP reporter induction in an unwounded wild-type embryo. Selected frames from the movie are presented in Fig. S1C

Supplementary Movie 2. Time-lapse movie showing the *Ddc1.4*-GFP induction in a wild-type embryo after wounding. Recording started immediately after embryo wounding. Selected frames from the movie are presented in Fig. S1D

Supplementary Movie 3. Confocal time-lapse movie showing epidermal wound re-epithelialization in a wild-type embryo expressing *sqh*-GFP moe. Wound closure takes 90 minutes.

Supplementary Movie 4. Confocal time-lapse movie showing epidermal wound re-epithelialization in a *src42Abtk29A* mutant embryo expressing *sqh*-GFP moe. The actin-cable around the wound is weak, discontinues and the wound remains open for at least 300 min after wounding.